Langmuir
Article
pubs.acs.org/Langmuir

Particle Capture via Discrete Binding Elements: Systematic Variations in Binding Energy for Randomly Distributed Nanoscale Surface Features

Surachate Kalasin,[†] Surangkhana Martwiset,[‡] E. Bryan Coughlin,[†] and Maria M. Santore*,[†]

[†]*Department of Polymer Science and Engineering, University of Massachusetts, 120 Governor's Drive, Amherst, Massachusetts 01003, United States.* [‡]*Current address: Department of Chemistry, Khon Kaen University, Thailand*

Received July 29, 2010. Revised Manuscript Received September 24, 2010

This work examines how the binding strength of surface-immobilized "stickers" (representative of receptors or, in nonbiological systems, chemical heterogeneities) influences the adhesion between surfaces that are otherwise repulsive. The study focuses on a series of surfaces designed with fixed average adhesive energy per unit area and demonstrates quantitatively how a redistribution of the adhesive functionality into progressively larger clusters (stronger stickers) increases the probability of adhesive events. The work employs an electrostatic model system: relatively uniform, negative 1 μm silica spheres flow gently over negative silica flats. The flats contain small amounts of randomly positioned nanoscale cationic patches. The silica−silica interaction is repulsive; however, the cationic patches (present at sufficiently low levels that the overall surface charge remains substantially negative) produce local attractions. In this study, the attractions are relatively weak so that multiple patches engage to capture flowing particles. Experiments reveal an adhesion signature characteristic of a renormalized random distribution when the sticker strength is increased at an overall fixed binding strength per unit area of surface. The form of the particle capture curves are in good quantitative agreement with a simple model that assumes only a fixed adhesion energy needed for particle capture. Aside from the quantitative details that provide a simple formalism for anticipating particle adhesion, this work demonstrates how increasing the heterogeneities in the surface functionality can cause a system to go from being nonadhesive to becoming strongly adhesive. Indeed, systems containing small amounts of discretized adhesive functionality are always more adhesive than systems in which the same functionality is distributed uniformly over the surface (the mean field scenario).

Introduction

Discrete binding events distinguish ligand−receptor systems (such as cell-adhesion molecule-mediated bioadhesion, multivalent drug-targeting packages, and DNA and immunoassay chips) from the conceptualized interfaces forming the basis for classical adhesion theory and interfacial physical chemistry (colloidal interactions). The latter assume that surfaces are featureless and uniform. Classical adhesion theory assigns adhesion energy on a per area basis so that adhesion strength increases linearly with contact area. The classical field of interfacial physical chemistry does likewise: van der Waals and electrostatic interactions are calculated by employing descriptors of average surface properties such as the surface potential or Hamaker constant. From these, flat plate interactions are calculated or expressions for geometry-specific forces and energies are developed.[1]

Discrete binding groups potentially produce dynamically complicated adhesive behavior. For example, the underlying binding kinetics of individual ligand−receptor pairs or diffusional processes that bring a ligand within range of a receptor can impart time dependence and history dependence.[2] Such diffusion- and reaction-limited kinetics have been identified by Noppl-Simson[3] and Boulbitch[4] using model vesicles functionalized with adhesive molecules. Lag times and interfacial instabilities result in the extreme when the energy of slow binding competes with that of interfacial deformation.[5] These behaviors are complicated by the clustered presentation of ligands/receptors in the unbound state, which can produce dynamic binding cooperativity. Similarly complex behavior is expected on living cells.

A thermodynamic consequence of localizing attractive interactions into discrete binding groups is the altered binding equilibrium compared with a uniform surface. Indeed, the use of many small binding elements rather than a single large one facilitates multivalent binding, a strategy frequently exploited in pharmaceutical chemistry:[6] multivalency shifts the binding equilibrium in a power law fashion relative to single binding events and increases selectivity accordingly.[7] Indeed, the enhancements associated with multivalent binding recur in nature, for instance, the action of antibodies and other workings of the immune system.[8]

Beyond the discrete ligand−receptor interactions found in biology, most natural nonbiological systems exhibit interfacial heterogeneity that can serve to localize attractive interactions discretely or nearly so. Systems with such interfacial heterogeneity, for instance, electrostatic systems, are poorly approximated by classical approaches such as DLVO (Derjaguin, Landau, Verwey, and Overbeek) because the appropriate descriptors of average surface properties are not the area-averaged values that are conventionally employed (e.g., surface or zeta potential.) As an example, it is common to find electrostatic attractions between

(1) Israelachvili, J. *Intermolecular and Surface Forces*; Academic Press: Boston, 1992.
(2) Jeppesen, C.; Wong, J. Y.; Kuhl, T. L.; Israelachvili, J. N.; Mullah, N.; Zalipsky, S.; Marques, C. M. *Science* **2001**, *293*, 465–468.
(3) NopplSimson, D. A.; Needham, D. *Biophys. J.* **1996**, *70*, 1391–1401.
(4) Boulbitch, A.; Guttenberg, Z.; Sackmann, E. *Biophys. J.* **2001**, *81*, 2743–2751.
(5) Nam, J.; Santore, M. M. *Langmuir* **2007**, *23*, 10650–10660.
(6) Kiessling, L. L.; Gestwicki, J. E.; Strong, L. E. *Curr. Opin. Chem. Biol.* **2000**, *4*, 696–703.
(7) Kitov, P. I.; Bundle, D. R. *J. Am. Chem. Soc.* **2003**, *125*, 16271–16284.
(8) Pluckthun, A.; Pack, P. *Immunotechnology* **1997**, *3*, 83–105.

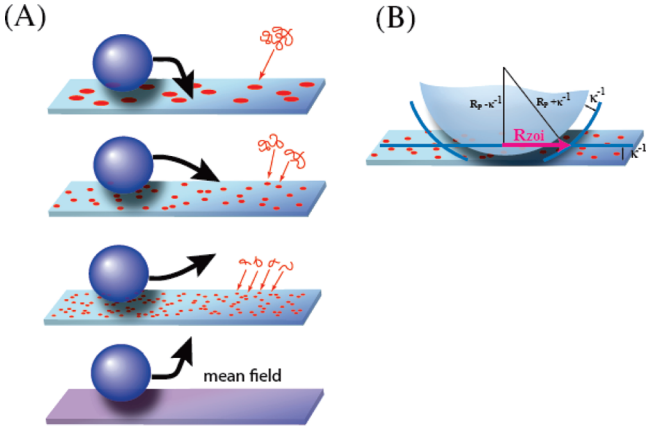

Figure 1. (A) Schematic demonstrating the redistribution of cationic adhesive functionality (red) on a repulsive negative surface (blue) through changes in the size of nanoscopic cationic patches. The series keeps the amount of the cationic functionality on the surface constant. In the limit of extremely small cationic functionality compared with all other length scales, the average (or mean field) surface characteristics are relevant. Negative microparticles adhere to surfaces with larger patches and the same overall cationic functionality but are nonadherent on the mean field surface or surfaces with small clusters of charge. (B) Effective electrostatic contact area (zone of influence) determined by the Debye length. The radius of the zone of influence, $R_{zoi} = 2\ (\kappa^{-1}R_p)^{1/2} = 63.25$ nm, for the ionic conditions in this study.

surfaces that carry the same net surface charge and should therefore be repulsive under the particular ionic conditions of study. This occurs in electrostatically driven mineral aggregation,[9−11] in membrane fouling,[12,13] and in bacterial adhesion to negatively charged surfaces[14−16] because the highly positive regions on one surface attract negative regions on the opposing surface. Elimelech developed a quantitative treatment of electrostatically heterogeneous systems employing a surface-potential-like parameter that anticipated the correct interactions[17] but depended on properties such as ionic strength in ways that were not clearly associated with a physical mechanism. The Adamczyk group also explored the role of charge heterogeneity and roughness in the capture of flowing particles, demonstrating a capture threshold effect that was also seen by us.[18,19] More recently, Santore and Davis demonstrated how the length scales within the random distribution of discrete surface groups, relative to other length scales such as a contact radius, determined interfacial forces and net particle interactions.[20] Here the important parameters were the surface potentials of the two surface functionalities and their surface densities.

The current work elaborates further on adhesion driven by localized attractions or nanoscale adhesive groups ("sticky patches") on surfaces whose underlying physical chemistry is mutually repulsive. The regime of interest is that where the average character of both surfaces is also negative, so DLVO theory anticipates substantial long-range repulsions. Instead of repulsions, however, attractions are observed to dominate and produce adhesion, even with extremely low densities of sticky patches or small areas of adhesive functionality. This article focuses on variations in the binding energy per adhesive element, keeping constant the overall average surface properties such as charge/area (or adhesion energy/area), as illustrated in Figure 1. The system is chosen to eliminate kinetic effects related to the binding events themselves, for instance, those that might occur with a series of ligand−receptor pairs. In this way, we examine the impact of redistributing the attractive surface charge, a process analogous, in other systems, to the clustering of bioadhesive functionality. Experimental results are compared with a simple model that demonstrates the role of spatial fluctuations in adhesion and how adhesion probabilities are renormalized with the strength of the heterogeneity.

Development of the Model Experimental System

This study employs negative silica surfaces decorated with small amounts of adsorbed cationic polymer (the adhesive component), which enables the capture of flowing silica microspheres. At low surface densities of the adsorbed polycation, individual chains act as adhesive patches that are isolated from one another and randomly distributed.[18,19] The negative charge on the silica particles and on the main surface of the collector produces a substantial electrostatic repulsion against which the patch−sphere electrostatic attractions compete.

Notably, a fully saturated adsorbed polycation layer, of the type that we employ, overcompensates for the underlying charge of the silica substrate.[21] Thus, single polycation chains, isolated from each other by relatively large areas of bare surface, represent patches of positive surface charge. Higher-molecular-weight chains contain greater numbers of positive charge than short chains and therefore localize a greater number of positive charges in a somewhat larger but still locally concentrated region of the surface than do short chains. A key strategic component of the current study, when the adsorbed mass per area of the polycation is fixed, is that the overall charge on the surface is also constant. (This experimental design element will be substantiated in the Results section.) Variations in the polycation molecular weight merely redistribute the charge on the surface, per Figure 1. Although increasing the molecular weight of the polycation increases the patch area, we argue below in the Results and Discussion sections that the binding energy per patch, also proportional to the molecular weight, rather than the patch size is the critical consideration for particle capture.

A large body of our previous work established a model system for electrostatically heterogeneous surfaces based on one polycation, pDMAEMA (poly(dimethylaminoethyl methacrylate)), sample.[18−22] The three additional molecular weight samples in this article are expected to exhibit the same qualitative features when deposited on silica surfaces. (Strategic points in the experimental design are described here, with the appropriate features substantiated in the Results section.) First, the cationic patches tend to be relatively flat because, as a general rule for densely charged polyelectrolytes adsorbing on an oppositely charged surface, the backbone adheres to the surface mostly in trains.[22,23] Next, the size of the patch, in terms of its surface footprint, is well

(9) Fuerstenau, D. W.; Pradip *Adv. Colloid Interface Sci.* **2005**, *114*, 9–26.
(10) Lagaly, G.; Ziesmer, S. *Adv. Colloid Interface Sci.* **2003**, *100*, 105–128.
(11) Tombacz, E.; Csanaky, C.; Illes, E. *Colloid Polym. Sci.* **2001**, *279*, 484–492.
(12) Zhu, X. H.; Elimelech, M. *Environ. Sci. Technol.* **1997**, *31*, 3654–3662.
(13) Leslie, G. L.; Schneider, R. P.; Fane, A. G.; Marshall, K. C.; Fell, C. J. D. *Colloids Surf., A* **1993**, *73*, 165–178.
(14) Walker, S. L.; Hill, J. E.; Redman, J. A.; Elimelech, M. *Appl. Environ. Microbiol.* **2005**, *71*, 3093–3099.
(15) Walker, S. L.; Redman, J. A.; Elimelech, M. *Langmuir* **2004**, *20*, 7736–7746.
(16) Truesdail, S. E.; Lukasik, J.; Farrah, S. R.; Shah, D. O.; Dickinson, R. B. *J. Colloid Interface Sci.* **1998**, *203*, 369–378.
(17) Song, L. F.; Johnson, P. R.; Elimelech, M. *Environ. Sci. Technol.* **1994**, *28*, 1164–1171.
(18) Kozlova, N.; Santore, M. M. *Langmuir* **2006**, *22*, 1135–1142.
(19) Santore, M. M.; Kozlova, N. *Langmuir* **2007**, *23*, 4782–4791.
(20) Duffadar, R. D.; Kalasin, S.; Davis, J. M.; Santore, M. M. *J. Colloid Interface Sci.* **2009**, *337*, 396–407.
(21) Shin, Y. W.; Roberts, J. E.; Santore, M. M. *J. Colloid Interface Sci.* **2002**, *247*, 220–230.
(22) Shin, Y.; Roberts, J. E.; Santore, M. M. *Macromolecules* **2002**, *35*, 4090–4095.
(23) Fleer, G. J.; Cohen Stuart, M. A.; Scheutjens, J. M. H. M.; Cosgrove, T.; Vincent, B. *Polymers at Interfaces*; Chapman and Hall: London, 1993.

represented by the free solution coil size, as determined by dynamic light scattering.[18,19] There is little expansion or collapse of the coil on adsorption, as expected given the strong nature of the electrostatic interactions that hold the chain in place.

It is also well established that pDMAEMA adsorbs strongly under the conditions of interest in the current study and does not desorb, diffuse, become displaced by other species, or transfer to particles encountering the interface.[18,19,24,25]

Experimental Materials and Methods

This study employed three different samples of pDMAEMA, poly(dimethylaminoethyl methacrylate), described in Table 1. Well-controlled polymerizations of pDMAEMAs were carried out via atom-transfer radical polymerization (ATRP). In a slight modification of a literature preparation,[26] a typical ATRP was carried out as follows: CuBr was placed into a dried ATRP tube. The tube was then flushed with dry N_2 for 15 min. The deoxygenated solvent mixture (isopropanol/water (9/1 v/v)), deoxygenated DMAEMA, and 1,1,4,7,10,10-hexamethyltriethylenetetramine (HMTETA) were added to the tube and then stirred until the system became homogeneous. Three cycles of freeze−pump−thaw were conducted, followed by the addition of *p*-TsCl (*p*-toluenesulfonyl chloride). Three more cycles of freeze−pump−thaw were performed. The solution was then stirred at room temperature. The molar ratio of CuBr/HMTETA/*p*-TsCl was 1/1/1, and the volume ratio of DMAEMA to the solvent mixture was 1/1. After polymerization, the residual copper catalyst was removed by passing the reaction mixture down a short column filled with basic alumina. The polymer solution was concentrated and precipitated in hexane. ^{1}H NMR (300 MHz) was conducted on a Bruker DPX-300 NMR spectrometer with the samples dissolved in chloroform-*d* to confirm their chemical structure. The molecular weight and polydispersity index (PDI) were measured by gel permeation chromatography (GPC) in DMF at 50 °C with a flow rate of 0.75 mL/min on systems equipped with two-column sets (from Polymer Laboratories) and a refractive index detector (HP 1047A). Poly(methyl methacrylate) standards were used for molecular weight calibration. Sample characterization data, along with the reaction scheme, is included in the Supporting Information.

Surfaces were prepared and particle capture was studied in pH 6.1 phosphate buffer (0.0234 M KH_2PO_4 with a very small amount of dilute NaOH solution added to adjust the pH.). Salts were purchased from Fisher Scientific. For this buffer, the ionic strength is 0.026 M, corresponding to a Debye length of 2 nm.

The patchy surfaces were created by adsorbing pDMAEMA from dilute (20 ppm) pH 6.1 buffered solution flowing gently (wall shear rate = 5 s^{-1}) over acid-etched microscope slides (Fisherfinest) in a slit-shear chamber. Reinjection of buffer after the adsorption period enabled tight control of the number of patches deposited, as previously established.[18] Soaking slides overnight in concentrated sulfuric acid and then thoroughly rinsing them in DI water is known to produce silica surface layers on the order of 10 nm thick.[27]

After the surfaces had been prepared, without being removed from the slit flow chamber they were exposed to 0.1 wt % suspensions of monodisperse 1 μm microspheres (GelTech, Orlando, FL) flowing at a wall shear rate of 22 s^{-1} in the same buffer. Particle accumulation was monitored using a custom-built lateral microscope employing a 20× Nikon objective focused at the interface between the functionalized surface and the solution. This instrument orients the surface of interest vertically so that gravity does not interfere with particle−surface interactions. Data were recorded at standard video rates. The field of view was 236 μm × 137 μm, with the 236 μm dimension being that for the flow. Data were recorded for approximately 10−20 min for each experiment.

Image J software was used to quantify the numbers of adherent particles at each time step. Because Image J counts all particles in focus, including those near the surface and moving past it, the free particle contribution to the signal was subtracted either by reinjecting buffer at the end of the run or by employing further analysis to discriminate moving particles.[28]

The adsorbed amounts of pDMAMEA at saturation and the adsorption kinetic curves used as a calibration of the deposition procedures mentioned above were determined by near-Brewster reflectometry, a method that is similar to ellipsometry but traces the adsorbed amount on a microscope slide in real time. In optical reflectometry, a HeNe laser, polarized parallel to the optical plane of incidence, is brought into the substrate from behind, near the Brewster angle. Here, the intensity of the reflected beam increases dramatically with the accumulation of material at the interface, with polycation adsorption scaling as the square root of the reflectometry signal after the subtraction of the optical background from the silica layer on the microscope slide.[27]

To facilitate zeta-potential studies of the average electrostatic character of the heterogeneous planar collecting surfaces, a dispersed system based on the 1μm silica microspheres (the same as above, from GelTech) was developed. Microparticles were suspended at a concentration of 250 ppm in pH 6.1, I = 0.026 M phosphate buffer, and varied amounts of pDMAEMA solutions were added dropwise from a 1 ppm pDMAEMA solution. After initial mixing, the solutions were allowed to equilibrate overnight with gentle stirring using a magnetic stir bar. Zeta potentials were measured on a Malvern Zetasizer Nano ZS instrument. Five measurements were made for each pDMAEMA concentration/molecular weight. We found the mixing procedure of combining the silica suspension with the pDMAMEA solution to be the best approach to obtaining stable dispersions, indicating a relatively uniform distribution of pDMAMEA among all the particles in a sample.

Results

Characterization of the System. To substantiate key points of the experimental strategy and to enable the creation of surfaces with tightly controlled amounts of pDMAEMA, studies of its adsorption on acid-etched microscope slides were first undertaken. The results are summarized in Table 1, with data provided in the Supporting Information. The saturation coverage, Γ_{sat}, of pDMAEMA on silica increases modestly with pDMAEMA molecular weight, an effect more pronounced at low molecular weights. When these coverages are converted to the excluded coil area, the first measure of patch size ($A_{coil} = M_w/\Gamma_{sat}$ * unit conversion), the increase in patch size with molecular weight is evident. These estimates of the adsorbed coil footprint are in good agreement with dynamic light scattering measurements of the free coil size. Differences increase at higher molecular weight, suggestive of thicker adsorbed layers at elevated pDMAEMA molecular weight.

Figure 2, featuring the zeta potentials of 1 μm silica spheres with increasing adsorbed amounts of pDMAEMA, provides insight into the average electrokinetic character of the various collecting surfaces. As the amount of adsorbed polycation is increased, the zeta potential goes from being strongly negative ultimately to being substantially positive. Adsorbed pDMAEMA overcompensates for the underlying negative silica charge, as previously seen with a pDMAEMA sample of different molecular weight.[21] Next, when the full range of pDMAEMA coverage is considered, it becomes apparent that higher-molecular-weight chains are less effective at increasing the zeta potential than are lower molecular weight chains: the numbers of loops and tails, albeit tiny in these in polyelectrolyte layers adsorbed on surfaces of opposing charge,

(24) Hansupalak, N.; Santore, M. M. *Macromolecules* **2004**, *37*, 1621–1629.
(25) Santore, M. M. *Curr. Opin. Colloid Interface Sci.* **2005**, *10*, 176–183.
(26) Chatterjee, U.; Jewrajka, S. K.; Mandal, B. M. *Polymer* **2005**, *46*, 10699–10708.
(27) Fu, Z. G.; Santore, M. M. *Colloids Surf., A* **1998**, *135*, 63–75.
(28) Kalasin, S.; Santore, M. M. *Langmuir* **2010**, *26*, 2317–2324.

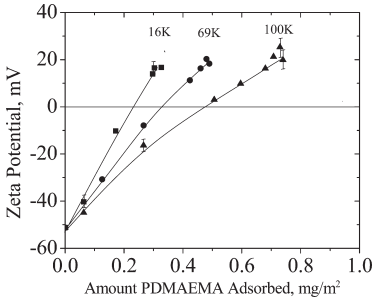

Figure 2. Zeta potentials of 1 μm silica spheres with different adsorbed amounts of pDMAEMA, in pH 6.1 phosphate buffer, with $I = 0.026$ M. Error bars show typical variations.

are larger for the higher-molecular-weight chains. This finding is consistent with differences in the effective adsorbed footprint and free coil size for the 100K molecular weight sample. Even small protrusions from an adsorbed layer push the shear plane outward dramatically.[23] Thus, the effect of the pDMAEMA molecular weight on the zeta potential is hydrodynamic in nature. One still expects that the amount of positive charge brought to the surface by pDMAEMA chains is proportional to the adsorbed mass, independent of molecular weight. Most relevant to the ability of the electrostatically patchy collecting surfaces to capture flowing microparticles are the zeta potentials, in Figure 2, near 0.1 mg/m^2 of pDMAEMA and below: in this range of adsorbed polycation loadings, the net surface charge is substantially net negative, close to that of bare silica.

As also pointed out by a reviewer, the ultimate coverages observed by reflectometry in Table 1 for each molecular weight of pDMAEMA adsorbed on a silica flat from a 20 ppm pDMAEMA solution differ from the apparent ultimate coverages in the suspensions of Figure 2. This modest difference, which is most important for the 100K pDMAEMA sample, likely results from the history dependence of the adsorption process: in reflectometry, the flowing bulk solution has a fixed concentration and the adsorbed amount increases progressively with time to saturation. In the zeta potential studies, a silica suspension and a polymer solution were mixed in proportion to give the desired surface coverage, assuming that all the polymer adsorbed. We mixed the suspension for a long enough time that we expected full adsorption to occur; however, in such a process, the bulk solution concentration decreases to nearly zero as the surface concentration of polymer increases. This complexity of approaching an extremely dilute bulk concentration in the suspension may give rise to the apparently higher calculated coverages corresponding to the positive zeta potentials in Figure 2. The effect, however, is modest and does not affect our take-home point concerning the general range of the zeta potential that is relevant to the particle-capture portion of the study.

Particle Capture. Figure 3 showcases the effect of polycation loading on the ability of the surfaces to capture 1 μm silica spheres. In these experiments, spheres flow over surfaces with different cationic patch loadings on the x axis. The accumulation rates of adherent particles are plotted on the y axis. Notably, these rates represent the steady-state adhesion of particles to each surface, that is, the linear region of sustained increase in particle number on the surface with time before the surface becomes sufficiently loaded with particles such that the accumulation rate is reduced. Example data in the Supporting Information emphasize the linearity.

For each of the three pDMAEMA molecular weights, the particle accumulation rate in Figure 3 increases with the surface loading of pDMAEMA patches starting not at the origin but with a unique x intercept for each pDMAEMA molecular weight. We term these x intercepts "adhesion thresholds," the minimum density of patches of a particular molecular weight needed for particle capture. Below each threshold, the surface contains an insufficient density of pDMAEMA patches for particle capture. This indicates that isolated single patches, even those composed of 100K molecular weight pDMAEMA, bind silica spheres too weakly for particle capture by a single patch.[18−20,29,30] Even with the larger 100K patches, several patches (at least two or three) engage during the capture of each microsphere. Therefore, roughly 20 chains of the 16K material at a minimum are engaged each time a particle is captured. Smaller (or more weakly binding) patches exhibit larger adhesion thresholds because greater numbers of small patches engage an arresting particle, compared to the number of large patches.

Also, toward the right-hand side of Figure 3A, all three data sets for the different molecular weights of pDMAEMA converge to a single particle capture rate corresponding to the transport-limited rate. The observed rate of 2.25 mg/m^2 min agrees with expectations from the Leveque equation,[18,31] given the silica particle concentration of 0.1 wt % and the particular flow geometry of our experiment. This upper bound on particle capture kinetics is observed for some surfaces containing relatively little pDMAEMA and indeed can be observed when the surfaces are slightly net negative. This indicates that once a particle is near the surface the time needed for it to diffuse away is greater than the time needed for it to find an adhesive region.

Because the chain molecular weight is directly proportional to the cationic functionality of the patches, Figure 3B considers the impact of patch mass concentration (rather than number concentration on the surface in Figure 3A) as the driving force for particle capture. The mass-based measure of the patch surface density incompletely collapses the three data sets for the different molecular weight patches onto each other. Rather than a perfect superposition, one finds a crossing of the data. For a fixed adsorbed pDMAMEA mass/area, the different molecular weight patches distribute the average interaction energy between the particle and the surface into different strength binding elements, with renormalized but random statistics. The crossing of the data in this fashion follows from the random statistical nature of the surface.

To see this more clearly, we model the distribution of sticky patches on the surface using a Poisson distribution that describes random arrangements, $P_{N_i}(x) = N_i^x e^{-N_i}/x!$, where the index i distinguishes the different molecular weight patches. N_i is the average number of a particular patch type, i, per unit area in the particle−surface contact region (defined in Figure 1B), x is a target number (potentially different from the average) of patches in the same area of particle−surface contact, and P is the probability of finding x given N_i. Notably, the average number N_i of patches per microscopic area of particle contact turns out to be the same as the macroscopic number-average patch loading on the x axis of Figure 3A.

Capture occurs when a particle encounters a region of surface containing a critical number N_i^* or more patches within the contact area. The probability of capture or adhesion, P_A, then sums the probabilities of a particle encountering a contact region with patch densities greater than the critical number:

$$P_A(N_i) = \sum_{x=N_i^*}^{\infty} P_{N_i}(x) \quad (1)$$

With the supposition that the total adhesive energy needed for particle capture is independent of patch size, the critical number of

(29) Adamczyk, Z.; Zembala, A.; Michna, A. *J. Colloid Interface Sci.* **2006**, *303*, 353–364.
(30) Adamczyk, Z.; Michna, A.; Szaraniec, M.; Bratek, A.; Barbasz, J. *J. Colloid Interface Sci.* **2007**, *313*, 86–96.
(31) Leveque, M. A. *Ann. Mines* **1928**, *13*, 284.

Table 1. Properties of the Three Samples of pDMAEMA, Adsorbed from a 20 ppm Solution

sample code	16K	69K	100K
molecular weight, M_w	16 300	69 100	100 300
polydispersity	1.10	1.12	1.14
Γ_{sat}, on SiO_2, mg/m^2 [a]	0.37	0.44	0.56
adsorbed coil diameter, nm $= A^{1/2}$	8.6 (A = 73 nm^2)	16.2 (A = 262 nm^2)	17.2 (A = 298.5 nm^2)
$2R_H$, from DLS	10	22	40

[a] At pH 6.1, I = 0.026 M.

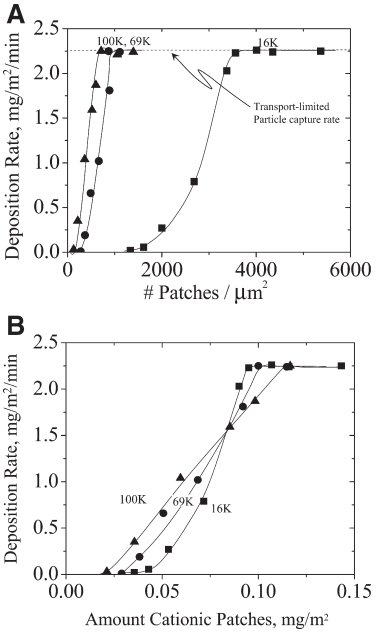

Figure 3. (A) Particle capture rates as a function of the areal density of adhesive patches on the surface. (B) Data from part A plotted in terms of the mass surface loading, which is representative of the average available binding energy per unit area.

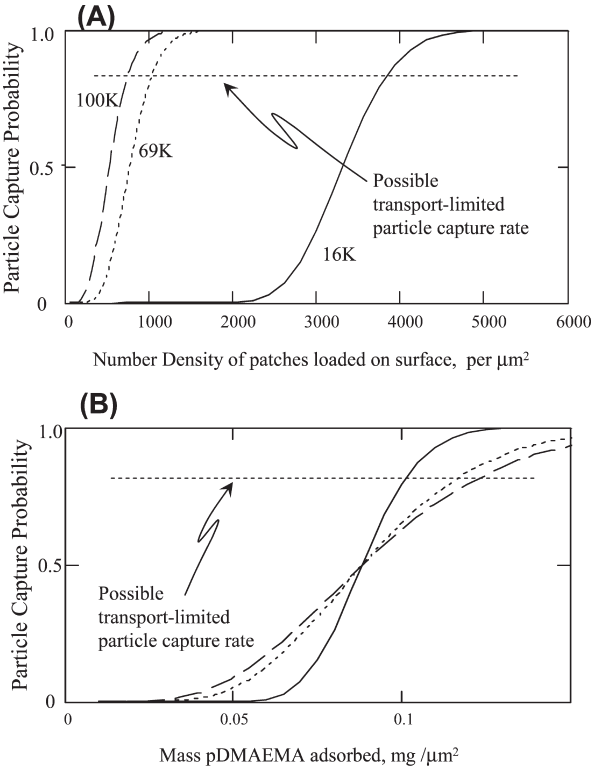

Figure 4. (A) Calculated capture probabilities as a function of patches/μm^2, with a capture criterion of 0.087 mg/m^2 in the zone of influence. (B) Calculations from plot A as a function of the mass loading of pDMAEMA on the surface.

patches N_i* becomes inversely proportionality to molecular weight. The single fitting parameter in the model, then, is the local mass concentration of polymer in the contact zone needed for particle capture. This parameter is applied once, and the particle capture rates for all pDMAEMA molecular weights and surface loadings follow. In fitting the model to the experimental data, we found 0.087 mg/m^2 to provide good results. One therefore estimates N_i* for the samples in this study according to

$$N_i^* = \pi R_{zoi}{}^2 \frac{0.087\ \text{mg/m}^2(1\ \text{g/mg})(6\times10^{23}/\text{mol})}{M_{w_i}(\text{g/mol})(10^6\mu\text{m/m})^2} \quad (2)$$

Figure 4A plots eq 1 for the three molecular weight patches in Table 1 using only eq 2 to specify the molecular-weight-dependent critical patch density. The x axis of Figure 4A divides N_i (the independent variable in eq 1) by the area of the contact zone between a 1 μm sphere and a flat plate for a Debye length of 2 nm ($\Pi R_{zoi}{}^2$ = 12 568 nm^2). The y axis of Figure 4A plots the probability of particle capture, which is related to the particle capture rate in an experimental system with many particles and many particle−surface encounters. The calculated plots quantitatively resemble the experimental observations of Figure 3A.

In Figure 4B, the calculation of Figure 4A is renormalized to produce a mass-based x axis representative of the average adhesive surface character. Differences in patch size now produce statistical effects on the probability of particle capture. Different numbers of patches (with different binding energies) must engage for patch capture, and the statistical probability of finding this multivalent interaction produces the crossing of the data, which is also observed experimentally.

Of note is that the calculations for Figure 4B show a crossing of the curves at midheight in the graph, corresponding to 50% probability. The crossing of the experimental data occurs higher on the graph. This is most likely because the experimental particle capture rates become transport-limited when particle−surface attractions become strong. Under these conditions, the intrinsic capture rate for the surface (i.e., corresponding to a high probability near unity) is not experimentally accessible.

Discussion

This article examines the impact of the binding strength of discrete binding surface elements on the capture of freely flowing particles. Randomly positioned binding sites are sufficiently small and their individual interactions with particles are sufficiently weak that many of them must engage for a particle to be captured (multivalency). It follows then that the number of engaged binding elements required for capture is inversely proportional to the binding strength or, in our experimental model, the molecular weight of the polycationic patch.

Although Figures 3A and 4A clearly demonstrate that when binding elements are weak, surfaces must be more densely loaded

with adhesive elements to facilitate microparticle capture, Figures 3B and 4B demonstrate that the average adhesive character of the surface (available binding energy per area) is not the sole consideration in particle capture. The statistics of the random distribution of the surface elements also comes into play. For surfaces having identical loadings of adhesive functionality (a fixed x-axis value), adhesion is favored when the adhesive chemistry is localized into relatively large "stickers" rather than smaller ones. Then the statistical fluctuation needed to bring a few strong adhesive elements into close proximity to one another is small compared to the spatial fluctuation needed to bring many weak elements into the particle−surface contact zone. This effect is apparent in the smaller adhesion thresholds with the higher-molecular-weight polymer in Figures 3B and 4B. It is also apparent that the trend becomes reversed when the surface becomes dense with adhesive elements. Here, particle capture occurs more readily at slightly smaller overall loadings of weak stickers.

Randomly placed discrete adhesive elements produce particle capture when the average surface character appears to be net repulsive toward particles, explaining a body of literature that speculates on the role of charge heterogeneity as the origin of unanticipated adhesive behavior.[14,15] This effect is most pronounced with strongly binding elements where the onset of adhesion at the threshold occurs at the lowest pDMAEMA mass coverage. Of note is the surface coverage of 0.087 mg/m^2 corresponding to the adsorbed polycation mass where the data cross represents the local density of adhesive functionality in the particle−surface contact region needed for adhesive capture. One can see this by imagining 0.087 mg/m^2 of pDMAEMA adsorbed on a series of surfaces employing chains of different molecular weights. When high-molecular-weight chains are employed, the positive charge is located in large polymeric islands separated by vast areas of negative surface. As the chain length is reduced, the number of islands increases and their center−center spacing decreases. In the limit of monomer distributed about the surface, the length scales between the surface functional groups become so small that all particle encounters with the surface are nearly the same: the spatial fluctuations on the surface become small over a length scale relevant to particle adhesion. The particle interaction with the conceptual monomer-treated surface becomes well-described by a mean field treatment. In this limit, the curves in Figures 3B and 4B would become step functions, intersecting with the curves for finite polycation polymers at 0.087 mg/m^2. The adhesion threshold of a step function is the same as the average surface character where adhesion turns begin. Therefore, the significance of the data crossing in Figure 3B is that it reveals the localized adhesive condition in the contact zone.

As an aside, it is worth mentioning that the appropriate measure of the average adhesive potential of the surfaces turns out to be the mass-based polycation adsorbed amount rather than the zeta potential (of the silica surface with its adsorbed pDMAEMA patches). The zeta potential is electrokinetic, sensitive to chain configuration, and predicts that similar adsorbed amounts of polycation, differing only in molecular weight, have different interfacial potentials. The development of the statistical model in Figure 4B assumes, and its good agreement with the experiments in Figure 3B suggests, that regardless of how chains are configured the binding energy per chain is proportional to its length (or number of cationic groups in the molecule). When a particle encounters a sticky patch made of an adsorbed polycation chain, all sections of the chain apparently have a nearly equal interaction with the approaching particle.

The physical scenario of surface-immobilized binding elements interacting with approaching particles is important, in general, because of the analogy to cell binding via cell adhesion molecules. Often in biological systems, cell adhesion molecules are up- or down-regulated and intercellular adhesion or signaling turns on or off. It becomes a natural question, then, if a certain number of bound adhesion molecules must engage for signaling, what level of up-relation (surface loading of the adhesion molecules) must be achieved? Figures 3B and 4B suggest a relationship between the required average surface loading of randomly distributed adhesion molecules and the probability of reaching the bound or on state. Although the division of adhesive energy among many weak elements imparts avidity,[6,7] there is a loss of overall binding when the positions of the binding elements are random. With randomly distributed elements, adhesion turns on at the lowest surface loadings of adhesion molecules when binding is strong.

Conclusions

An experimental model for particle capture and adhesion by discrete binding elements on a surface was developed using adsorbed cationic polymer coils on a negative surface. Systematic variation in the molecular weight of the polymer allowed an investigation of the binding energy per adhesive element. A comparison of particle capture on surfaces having the same mass loading of polymer but different molecular weight chains revealed the impact of the statistical distribution of adhesive functionality into discrete elements, keeping the overall adhesive energy per area of surface constant. Beyond the direct impact of the binding strength of the individual elements, the approach provided perspective on the differences between the adhesion of particles on uniform (mean field) surfaces and on surfaces with equivalent but discrete binding energy.

Comparing surfaces with equivalent average binding energies for approaching particles, it was demonstrated that clustering the adhesive functionality into strongly binding discrete units produced more extensive particle capture than did the distribution of the same adhesive functionality into a greater number of more weakly binding elements. Furthermore, it was possible to go from a nonadhesive to an adhesive state simply by redistributing the binding functionality into larger, more strongly adhesive elements. Finally, it was argued that surfaces containing randomly situated adhesive elements are always more adhesive than analogous surfaces with uniform character. (By analogous we mean surfaces where a fixed amount of adhesive functionality, such as the charge number, is smeared out over the surface as opposed to clustered.) Although these principles have been known from the biological perspective and applied in a qualitative fashion in multivalent drug targeting and bioadhesive surface design, this work provided a quantitative graphical relationship between mean field adhesive functionality and the adhesion achieved with discrete elements.

Acknowledgment. This work was supported by NSF CBET-0932719, CBET-0428455, and DMR-0820506. Additionally, access to the Zetasizer, within the UMass Center for Hierarchical Manufacturing, was made possible by NSF CMMI-0531171. S.M. thanks the Royal Thai Government for a graduate fellowship.

Supporting Information Available: Reaction scheme for the polymerization of pDMAEMA. ^{1}H NMR spectrum of 69K pDMAEMA with a molecular weight of 69K. Adsorption kinetic traces, via reflectometry, for the three pDMAEMA samples. Raw data for the deposition of 1 μm silica spheres at a shear rate of 39 s^{-1} onto silica flats with different patch loadings of 16 M_w pDMAEMA. This material is available free of charge via the Internet at http://pubs.acs.org.